LPP EUV Source Development for HVM

David C. Brandt*, Igor V. Fomenkov, Alex I. Ershov, William N. Partlo, David W. Myers, Norbert R. Böwering, Alexander N. Bykanov, Georgiy O. Vaschenko, Oleh V. Khodykin, Jerzy R. Hoffman, Ernesto Vargas L., Rodney D. Simmons, Juan A. Chavez, Christopher P. Chrobak
Cymer Inc, San Diego, CA 92127, USA

ABSTRACT

This paper provides a detailed review of development progress for a laser-produced-plasma (LPP) extreme-ultra-violet (EUV) source with performance goals targeted to meet joint requirements from all leading scanner manufacturers. We present the latest results on drive laser power and efficiency, source fuel, conversion efficiency, debris mitigation techniques, multi-layer-mirror coatings, collector efficiency, mass-limited droplet generation, laser-to-droplet targeting control, and system use and experience. The results from full-scale prototype systems are presented. In addition, several smaller lab-scale experimental systems have also been constructed to test specific physical aspects of the light sources. This report reviews the latest experimental results obtained on these systems with a focus on the topics most critical for a source intended for use in high volume manufacturing (HVM). LPP systems have been developed for light-sources applications to enable EUV scanners for optical imaging of circuit features at nodes of 32 nm and below on the international technology roadmap for semiconductors (ITRS). LPP systems have inherent advantages over alternate source types, such as discharge produced plasmas (DPP), with respect to power scalability, source etendue, collector efficiency, and component lifetime. The capability to scale EUV power with laser repetition rate and pulse energy is shown, as well as the modular architecture for extendability. In addition, experimental results of debris mitigation techniques and witness sample lifetime testing of coated multi-layer-mirrors (MLM) are described and used to support the useful lifetime estimation of a normal incidence collector. A roadmap to meet requirements for production scanners planned well into the next decade is also presented.

Keywords: EUV source, EUV lithography, Laser Produced Plasma, High Volume Manufacturing

1. INTRODUCTION

EUV Lithography is currently slated as the next critical dimension imaging solution after 193 nm immersion lithography below the 32 nm node on the ITRS beginning in 2013. Some forms of memory devices, such as NAND Flash may need the manufacturing technology as soon as 2011, with Beta generation systems required for development as early as 2009. The availability of a high power source for 13.5 nm radiation has been categorized as high risk and ranked with other technologies requiring significant developments to enable the realization of EUV lithography. Photoresist performance parameters needing the greatest amount of development include sensitivity or speed, line-edge-roughness (LER), and line-width-roughness (LWR). Photoresist sensitivity and other light absorbing materials are the basis to derive EUV source power requirements within the usable bandwidth (BW) of 2 %. According to the joint requirements from scanner manufacturers an EUV power of >115 W in 2 % BW at the intermediate focus (IF) is required for 5 mJ/cm^2 photoresist speed to enable >100 wph scanner throughput, and 180 W in 2 %BW at IF is needed for 10 mJ/cm^2. Photoresist sensitivities above 20 mJ/cm^2 could drive power requirements well above the 200 W level, and therefore, a scalable EUV source architecture is needed to enable the evolution of EUV lithography during the life cycle of the technology. Low power discharge-produced-plasma sources have been credited with the capability of producing 10 W at IF and are expected to be scalable to the 30 W - 50 W range. Laser-produced-plasma sources, on the other hand, are expected to deliver the necessary high power for critical-dimension high-volume manufacturing scanners for the production of integrated circuits in the post-193 nm immersion era.

LPP EUV lithography light sources generate the required 13.5 nm radiation by depositing laser energy into a source element, such as xenon (Xe), tin (Sn) or lithium (Li), creating a highly ionized plasma with electron temperatures of

*dbrandt@cymer.com

Emerging Lithographic Technologies XI, edited by Michael J. Lercel,
Proc. of SPIE Vol. 6517, 65170Q, (2007) · 0277-786X/07/$18
doi: 10.1117/12.713279

several 10's of eV. The energetic radiation generated during de-excitation and recombination of these ions is emitted into all directions. It is collected with a normal-incidence mirror (collector), and focused to an intermediate point from where it is relayed to the scanner optics and ultimately to the wafer. The conversion efficiency (CE) of the laser energy into EUV energy is critical to meeting the required power levels. Previously, we have investigated and discussed several combinations of laser wavelength and source element with respect to CE and other aspects of light source integration[1]. In this report we focus on the combination of CO_2 laser radiation and Sn droplet targets. A prototype configuration based on this approach is described and several recent developments are discussed. The normal incidence mirror is protected from the plasma by advanced debris mitigation technology. High-energy ions, fast neutrals, and residual source element particles are mitigated to maintain the reflectivity of the collector mirror and enable a long lifetime of this component. Metrology to measure the properties of light at both the plasma and IF are used to qualify the performance of the source.

2. LPP SYSTEM PROTOTYPE

The laser produced plasma development system at Cymer was reconfigured to include a high-power high repetition rate CO_2 laser in the second quarter of 2006 (see Figure 1). The output power was measured to be on the order of 3 kW at 30 kHz during the installation phase. In the late fourth quarter of 2006 the CO_2 laser system was upgraded to increase the output power to approximately 7 kW at 50 kHz.

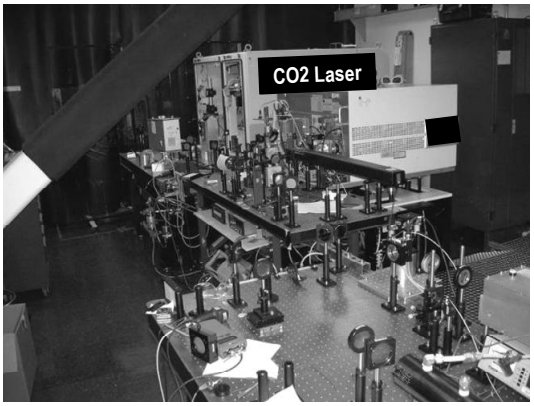

Figure 1: View of CO_2 laser system during installation.

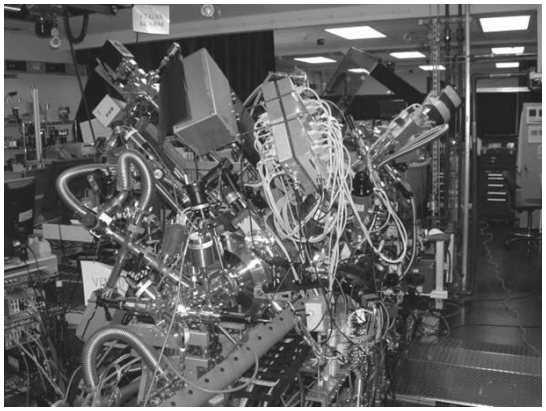

Figure 2: LPP chamber with Sn droplet capability.

The CO_2 laser is an axial-flow RF-pumped MOPA configuration with multiple stages of amplification. Its general layout was described previously[2]. The seed pulse is initiated by a Q-switched Master Oscillator (MO) with low energy and high repetition rate, capable of 100 kHz operation. The laser pulse is amplified, shaped, and focused before entering the LPP chamber (see Figure 2). The LPP chamber can be evacuated to approximately 10^{-6} Pa. The laser pulses are timed to an incoming liquid Sn droplet stream flowing from a target delivery system at a repetition rate comparable to or larger than the laser. Steering is provided to an exact point in the vacuum chamber where the droplet is irradiated by the laser beam. At the interaction region a plasma front with highly excited species is formed which radiates the desired 13.5 nm photons. A collector mirror can be installed to facilitate measurements of the power at IF at the output end of the source chamber.

The research and development system serves as the primary tool to test the fundamental capability and longevity of production designs. The performance is monitored by metrology directed at both plasma and at intermediate focus. A multi-location witness sample holder at the position of the collector is used to acquire life test data on various MLM samples allowing the effectivity of the debris mitigation and reflectivity of the MLM coatings to be evaluated quantitatively. Integrated controls permit automatic operation of the system as well as monitoring and data collection from the various metrology instruments on-board the LPP chamber.

3. RECENT DEVELOPMENT RESULTS

Starting from a prototype system level described a year ago[3], the main emphasis during the last LPP development campaigns at Cymer has been on achieving substantial gains of the source output power by continuous improvement of laser intensity generated on the target droplet. At the same time, the pulse repetition rate was also increased significantly. These improvements have led to a remarkable, 25-fold increase in IF-equivalent EUV 2 % in-band output power from the system over the course of the past year. This was achieved by a variety of pronounced advances in the areas of laser output power, laser beam quality, beam and pulse shaping and focusing optics. The IF-equivalent power is determined from the in-band EUV power measured at plasma using EUV monitors and a flying-circus-type detector with given input apertures at well-defined distances from the plasma, taking into account a collection angle of 5 sr, 50 % collector average reflectivity and 90 % transmission along the optical path from the plasma to IF. Figure 3 shows data obtained with the improved system during burst mode operation (5 bursts/s) at 40 kHz repetition rate on Sn droplets of 150 μm diameter. A sequence of 300 bursts of 1 ms length with the system in a free-running operation mode without active control is shown, producing IF-equivalent output powers of ~ 25 W. As another example, Figure 4 shows the results obtained during a period of 25 minutes at 50 kHz pulse frequency with > 25 W average IF power on smaller-size tin droplets (50 μm). In this case the mode of operation was 30 bursts/s with 50 pulses occurring in each burst. To ready the LPP source for HVM production conditions, a further increase of IF output powers to levels above 100 W is planned during the year 2007.

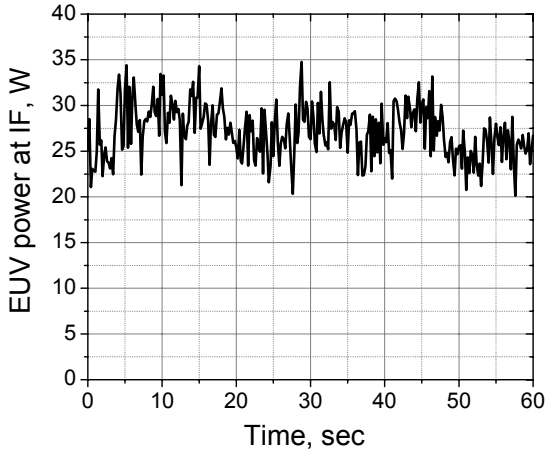

Figure 3: IF-equivalent output power vs. time for a sequence of 300 bursts during 40 kHz burst-mode operation with CO_2 laser focused on 150 μm diameter Sn droplets.

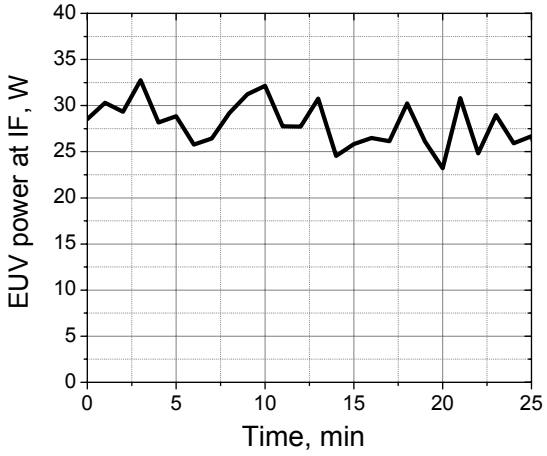

Figure 4: IF-equivalent inter-burst average output power vs. time at 50 kHz repetition rate. Operation was at 30 bursts/s and 50 pulses/burst for CO_2 laser focused on 50 μm diameter Sn droplets.

Extensive development efforts have been required to optimize the gas composition, gas pressure and RF power of the laser amplifier chain in order to achieve an amplification factor of ~2000x without suffering from amplified spontaneous emission (ASE). A balance between large small-signal gain and large saturation energy had to be reached in order to achieve high output power levels since these two parameters are inversely correlated[4]. Figure 5 shows the measured laser output power versus repetition rate of the master oscillator (MO). The laser pulse energy decreases from ~300 mJ/pulse at 10 kHz to ~150 mJ/pulse 50 kHz due to the gain depletion of the MO and amplifiers at the higher repetition rates. Work is continuing on increasing the laser output power to greater than 10 kW using novel architectures.

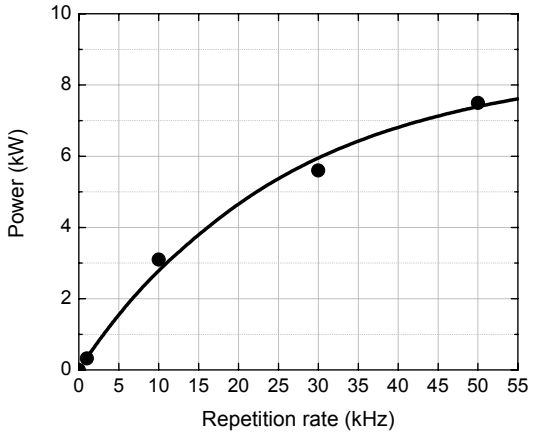

Figure 5: Measured laser power vs. repetition rate. The seed pulse is amplified approximately two thousand times after propagating through the amplifier chain.

The main requirements for the droplet generator are the capability to produce the tin droplets at a controllable frequency in the 20 – 200 kHz range with high droplet uniformity and stability and to provide a reliable operation over long periods of time. Recently, a third-generation version of the droplet generator was designed to fulfill these criteria. It represents a substantial performance improvement compared to earlier generators[5]. Figure 6a shows a photograph of the device. Stable droplets were obtained in a range of frequencies of 18 – 402 kHz with corresponding droplet diameters of 150 – 40 μm. Using a 10 μm nozzle tin droplets as small as 17 μm in diameter at a 550 kHz repetition rate have been demonstrated. Each droplet of this size has only ~ 10^{14} atoms, approaching the condition of the minimal mass required for efficient EUV generation. The total tin consumption in this high-frequency regime of operation is only 120 ml/day. When equipped with a small diameter nozzle the droplet generator is capable of producing stable tin droplets over extended periods of time. So far, 55 hours of continuous generator operation has been demonstrated, limited by the currently installed volume of tin supply.

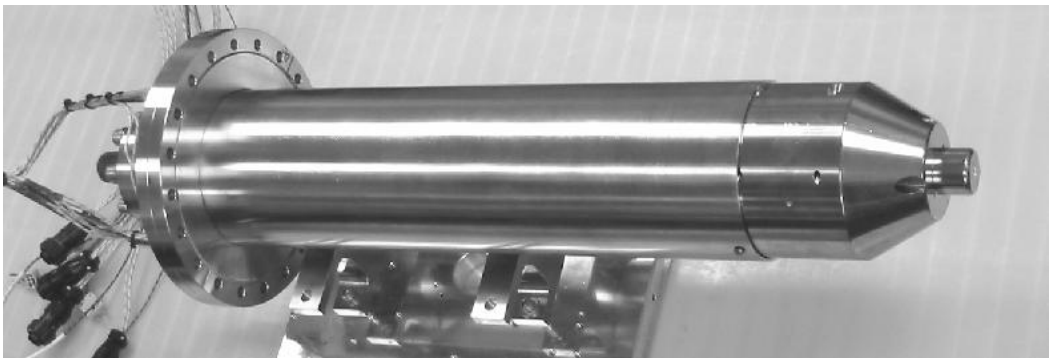

Figure 6: Third-generation liquid tin droplet generator consisting of heated Sn reservoir and nozzle.

The stability of the droplets produced by the droplet generator is determined by the nozzle design, by the parameters of the droplet generator (e.g., applied pressure and actuator driving voltage), and by the overall mechanical stability of the system. Using a modified nozzle design, substantial progress has recently been achieved with respect to the timing jitter of the droplets. A timing jitter of 25 ns (0.2 % of the droplet period) was demonstrated without using any active stabilization techniques. At the plasma location this corresponds to a spatial uncertainty of the droplet along the jet trajectory of ± 0.6 μm. The short term positional (transverse) stability of the droplets is on the order of 5 μm, whereas the long term (~ 15 minutes) stability is in the 100 μm range. The latter is routinely compensated by the active stabilization steering system.

The source chamber is equipped with a suite of metrology devices, including several photodiode-based in-band EUV power monitors of different designs, a grazing-incidence EUV spectrometer and an in-band EUV pinhole camera. These tools have been described in detail previously[6]. With the grazing-incidence spectrometer, the EUV portion of the spectrum emitted for the plasma was recorded during 15 kHz operation of the source. The normalized data for the region from 8 to 20 nm are shown in Figure 7. The peak emission of the CO_2-laser produced plasma occurs at 13.5 nm and matches well to the reflectivity curve of multilayer coated mirrors designed for this wavelength. The MLM curve displayed in the figure represents measured EUV reflectivity data for an interface-engineered high-temperature-stable coating with close to 60% peak reflectivity and more than 0.45 nm bandwidth (FWHM)[7]. In the EUV region, the coating acts as spectral purity filter reflecting mainly light near 13.5 nm. For the observed EUV spectrum the integrated out-of-band EUV radiation from 9 to 21 nm that is reflected by this coating amounts to only 3% of the reflected in-band EUV radiation. In contrast to previous spectra on Sn targets obtained at shorter drive laser wavelengths[6] the present spectrum recorded with CO_2 laser radiation does not show any indications of narrow absorption features. Rather, there are some narrow emission features in the long-wavelength side of the spectrum. This corroborates that the EUV emission is not limited significantly by the plasma opacity in this case.

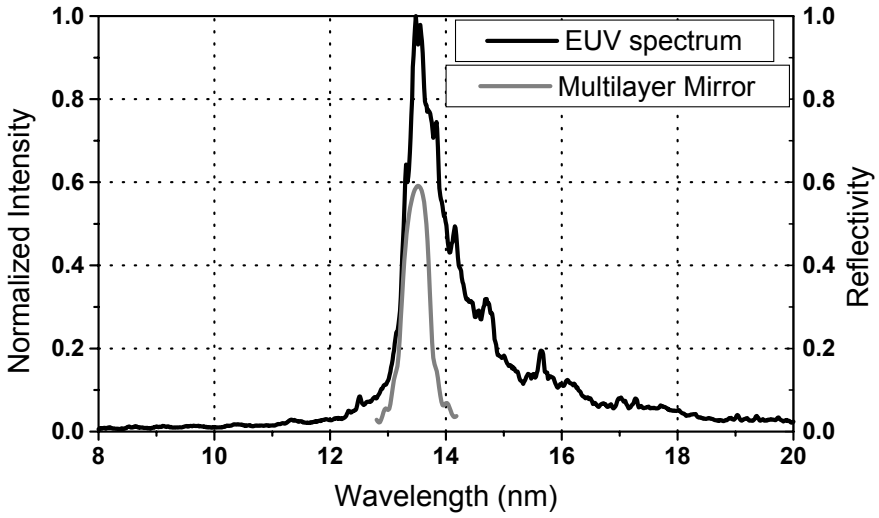

Figure 7: EUV spectrum for Sn droplets obtained with CO_2 drive laser during high-repetition-rate operation in comparison with high-temperature-stable MLM reflectance curve.

The size of the EUV emitting region of the micro plasma was measured using a pinhole camera arrangement viewing the plasma at an angle of 60° with respect to the laser beam direction. This device includes a reflection from a MLM and a Zr foil to record only in-band EUV emission[6]. Figure 8 shows data obtained when recording a burst of 50 pulses. The size of the region emitting radiation of 13.5 nm wavelength is typically ~120 μm in diameter. The plasma has overall cylindrical symmetry with respect to the optical axis with on-average ellipsoidal, near-spherical shape. This results in a small value for the etendue (~ 0.1 mm^2 sr) that can simplify the design of optical illumination devices thus enabling the implementation of high NA and high-throughput power systems.

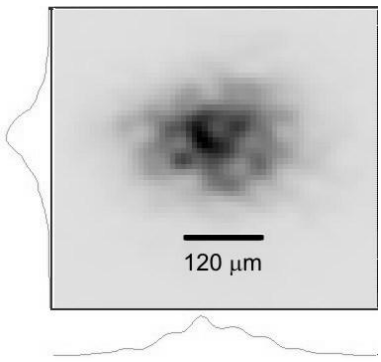

Figure 8: Typical pinhole camera image of in-band EUV source size for the case of CO_2 laser / Sn droplet target.

4. NORMAL INCIDENCE COLLECTORS

In our light-source configuration the laser beam is focused through a central opening of the collector mirror onto the droplet target for plasma generation. The EUV radiation emitted in the backwards direction is reflected at near-normal incidence by the ellipsoidal mirror and focused to the IF[8]. An advantage of this configuration is that a massive collector shell with large thermal load capacity and low deformation potential can be employed that is controlled by thermal management from the backside. A schematic view of this scheme is shown in Figure 9. The complete infrastructure was developed for manufacturing of large-size normal-incidence collector mirrors. For demonstration of the light collection capabilities of our source a 1.6 sr sub-aperture version (300 mm optical diameter) of the full HVM design with 5sr collection angle was implemented. After machining and super-polishing, the mirror surface was coated using a deposition tool and a technology based on dc magnetron sputtering compatible with large-area collector coating. A graded high-temperature-stable coating with interface-engineered multi-layers was applied to provide high EUV reflectivity at varying angle of incidence[7].

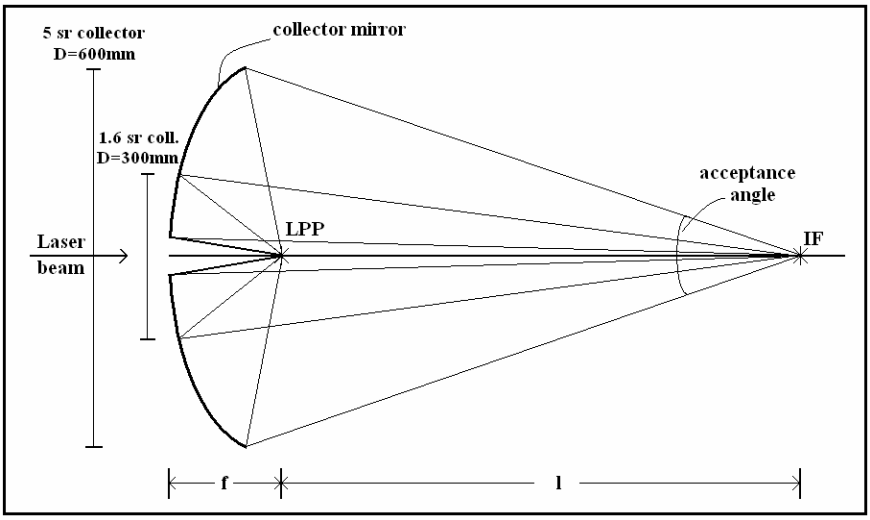

Figure 9: Light collection configuration with sub-aperture (1.6 sr) or full-aperture (5 sr) mirror.

The collector mirror was installed in the vacuum chamber and in use during 8 months on our LPP source when operated with a XeF drive laser[3]. In this time period the system was used extensively and modified several times while undergoing frequent heating and venting cycles. The peak reflectance of the mirror was measured with synchrotron radiation before and after this development period (PTB, Berlin). Figure 10 displays the reflectance values for a series of measurement points at increasing distance from the mirror center. The initial values before use were around

R = 40 %. After exposure, the reflectance decreased by about a factor of 2. However, after off-line cleaning with simple optical cleaning techniques the initial values were recovered, as found by another set of reflectance measurements.

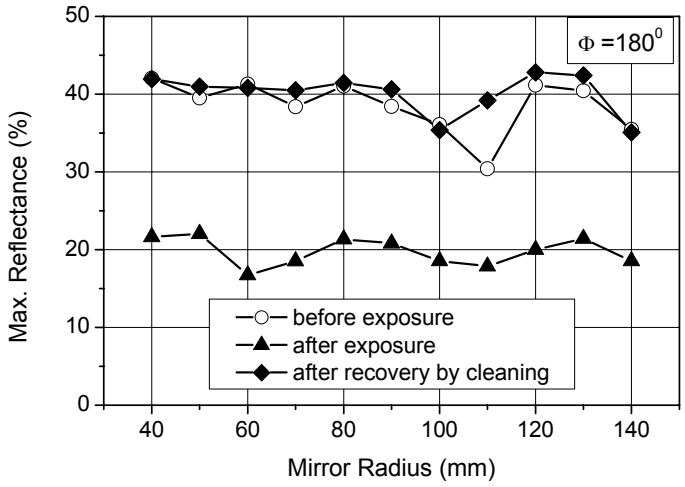

Figure 10: Measured EUV peak reflectance of collector mirror as a function of radius at 180° azimuthal angle before use, after use and after cleaning.

5. DEBRIS MITIGATION

LPP EUV sources generate debris impacting on the surface of the collector in the form of high-energy ions, neutral atoms and clusters of target material. Of these three types of debris the most hazardous for the collector mirror coating is the ion flux. The amount of neutral atoms and clusters from the droplet target impinging onto the collector is small since most of the target material moves in a direction pointing away from the collector surface. The efficiency of the developed in-situ cleaning technique is high enough to keep the surface of the collector free from Sn deposition.

The interaction of ions with energies of around a few kilo-electron volts with the surface results in erosion of the material of the MLM coating. To determine the erosion rate an experiment was conducted with the laser operating in burst mode under the same conditions as during EUV output power measurements. As discussed in a previous paper[3], the sputter depth can be characterized by quantitative SIMS analysis of multilayer samples if the layer number is not too high. The MLM samples with 8 bilayers and one capping layer were installed at the collector position and exposed to 19 Mpulses of LPP during source operation with IF equivalent in-band output power of more than 20 W. After the exposure the samples were analyzed using depth profiling by secondary ion mass spectrometry (SIMS, Millbrook Scientific Instruments PLC). The results are shown in Figure 11. The data indicate an erosion rate of ~ 0.2 layers per million pulses. This layer removal is attributed to sputtering during impact of energetic particles emitted from the plasma.

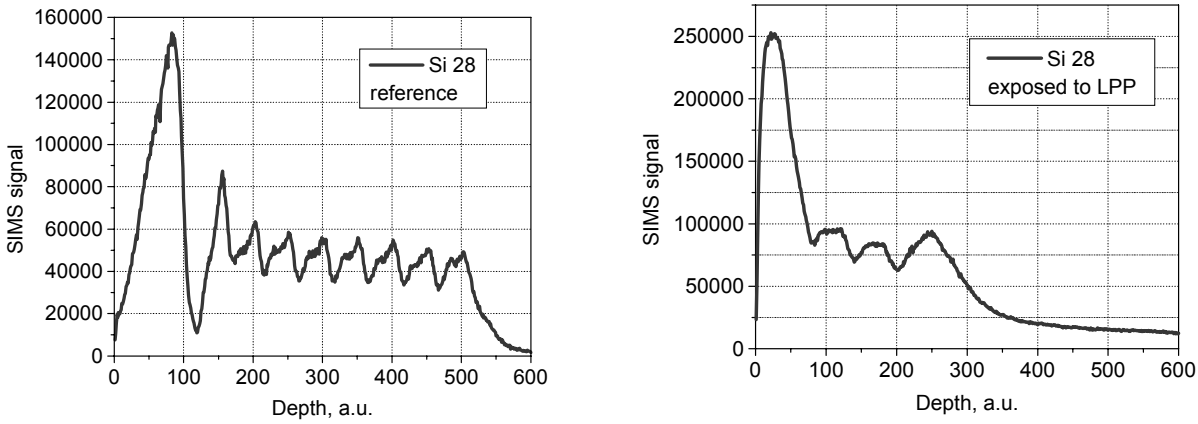

Figure 11: Lifetime test results for 8-layer sample without debris mitigation technique. a) SIMS depth profile of a MLM reference sample and b) SIMS profile of a sample after exposure to 19 M pulses. The reference sample shows 9 sputter peaks whereas the exposed sample shows 4.

For lifetime extension of the collector a mitigation technique for the energetic ions has been developed and tested[9]. The developed ion mitigation technique provides a suppression of the ion flux (i. e., the energy-integrated signal) by 4 orders of magnitude. Moreover, the maximum observed ion energy in the spectrum is lowered from 3 keV to < 300 eV. The collector mirror coating can have ~ 500 sacrificial layers and still provide full EUV reflectivity. Taking into account the measured erosion rate of 0.2 layers/Mpulses and the suppression factor of 10^4, a collector lifetime exceeding 10^{12} pulses is estimated. This corresponds to about 1 year of operation of the collector mirror. This estimation is based on flux reduction only. The observed significant decrease of maximum and peak ion energies will result in a further increase of the protection efficiency.

6. ROADMAP

The LPP source roadmap is shown in Figure 13. The generation 1 product is expected to meet requirements for pre-production or beta generation scanners in 2009. For this product the in-band EUV output power is targeting 100 W using a 10.8 kW CO_2 laser system on Sn droplets with 3.0 % conversion efficiency. The normal incidence collector used will have 5 sr of collection with a coating with an average EUV reflectivity approaching 50 %. Transmission losses due to obscurations, absorption, and debris mitigation techniques are projected to be less than 10 %. In line with the expected requirements for increased in-band EUV power at IF the second and third generation LPP EUV sources will be brought to market using 15 kW and 16 kW CO_2 laser technology with moderate improvements in CE and collection efficiency. It is expected that the time between insertion of generation nodes will be approximately twenty four months.

LPP EUV Performance Roadmap				
	Current	**Gen 1**	**Gen 2**	**Gen 3**
Laser power (kW)	**6.0**	**10.8**	**15.0**	**16.0**
In-band CE	1.5%	3.0%	3.5%	4.0%
Collecting angle (sr)	5	5	5	5.5
Collector average reflectivity	50%	50%	50%	50%
Optical transmission	90%	90%	90%	90%
Total power at IF (W)	**>25**	**100**	**165**	**225**
		- Equivalency assumption		

Figure 13: Projected LPP EUV source roadmap.

7. SUMMARY

Laser-produced plasma has been shown to be a viable source technology with scalability to meet requirements from leading scanner manufacturers and provide a path toward higher power as the lithography tools evolve over their life cycle. EUV powers exceeding 25 W at intermediate focus have been reported. An ion suppression debris mitigation technique was shown to have a measured suppression factor of 10^4 for normal incidence collectors. Experiments using coated witness samples have been performed to estimate the lifetime of the collector coating and have shown the feasibility to reach 10^{12} pulses. A sub-aperture normal-incidence collector mirror of 320 mm diameter with high-temperature graded multi-layer coating has been developed. The high-conversion-efficiency combination of 10.6 μm laser radiation and Sn source element has been described with CE well in excess of 4 %. The high CE values in our roadmap allow high EUV power at relativity low laser power to enable low cost operation to meet the expectations of chipmakers. EUV lithography is expected to be the critical dimension imaging solution post 193 nm immersion in 2011. LPP source technology is the most viable solution to enable the IF power requirement projected in the future and to provide the much needed margin in photoresist sensitivity, optics degradation, process latitude, and overall equipment throughput. Cymer currently plans commercialization of an EUV light source in 2009. Cymer continues to meet our EUV source development commitments to industry with demonstrations of >12 W in Q3 06 and >25 W in Q4 06. CO_2 on Sn droplets laser-produced plasma is our chosen technology path. High conversion efficiency is the key to cost effective solutions. High power high repetition rate CO_2 laser technology has been validated and is operational at above the 6 kW level. Current performance on our LPP development system is 75-90 W at plasma or 25-30 W equivalent at IF.

ACKNOWLEDGEMENTS

The authors gratefully acknowledge the valuable contributions from Martin J. Neumann, Brian E. Jurczyk and David N. Ruzic of University of Illinois – Urbana Champaign, Sergiy Yulin, Nicolas Benoit, Torsten Feigl and Norbert Kaiser of Fraunhofer Institut f. Angewandte Optik und Feinmechanik, Eric Gullikson and Franklin Dollar of Lawrence Berkeley National Laboratory and Martin Richardson of University of Central Florida. We are also very thankful for the invaluable support and contributions, past and present, of many scientists, engineers and technicians involved in the EUV technology program at Cymer.

REFERENCES

[1] B. A. M. Hansson, I. V. Fomenkov, N. R. Böwering, A. I. Ershov, W. N. Partlo, D. W. Myers, O. V. Khodykin, A. N. Bykanov, C. L. Rettig, J. R. Hoffman, E. Vargas L., R. D. Simmons, J. A. Chavez, W. F. Marx, D. C. Brandt, in: *Proc. of SPIE Vol. **5751**, Emerging Lithographic Technologies IX*, R. S. Mackay, Ed., 248-259 (2005).

[2] I. V. Fomenkov, B. A.M. Hansson, N. R. Böwering, A. I. Ershov, W. N. Partlo, V. B. Fleurov, O. V. Khodykin, A. Bykanov, C. L.Rettig, J. R. Hoffman, E. Vargas L., J. A. Chavez, W. F. Marx, D. C. Brandt, in: *Proc. of SPIE Vol. **6151**, Emerging Lithographic Technologies X,* M. J. Lercel, Ed., 61513X, (2006).

[3] B. A. M. Hansson, I. V. Fomenkov, N. R. Böwering, A. I. Ershov, W. N. Partlo, D. W. Myers, O. V. Khodykin, A. N. Bykanov, C. L. Rettig, J. R. Hoffman, E. Vargas L., R. D. Simmons, J. A. Chavez, W. F. Marx, D. C. Brandt, in: *Proc. of SPIE Vol. **6151**, Emerging Lithographic Technologies X,* M. J. Lercel, Ed., 61510R, (2006).

[4] L.M. Frantz, J. S. Nodvik, J. Appl. Phys. **34**, 2346 (1963).

[5] J. M. Algots, O. Hemberg, A. Bykanov, in: *Proc. of SPIE Vol. **5751**, Emerging Lithographic Technologies IX*, R. S. Mackay, Ed., 248-259 (2005).

[6] N. R. Böwering, J. R. Hoffman, O. V. Khodykin, C. L. Rettig, B. A. M. Hansson, A. I. Ershov, I. V. Fomenkov, in: *Proc. SPIE **Vol. 5752**, Metrology, Inspection, and Process Control for Microlithograpy XIX,* R. M. Silver, Ed., 1248-1256 (2005).

[7] T. Feigl, S. Yulin, N. Benoit, N. Kaiser, N. R. Böwering, A. I. Ershov, O. V. Khodykin, J. W. Viatella, K. A. Bruzzone, I. V. Fomenkov, D. W. Myers, in: *Proc. of SPIE Vol. **6151**, Emerging Lithographic Technologies X,* M. J. Lercel, Ed., 61514A, (2006).

[8] N. R. Böwering, A. I. Ershov, W. F. Marx, O. V. Khodykin, B. A. M. Hansson, E. Vargas, J. A. Chavez, I. V. Fomenkov, D. W. Myers, D. C. Brandt, in: *Proc. of SPIE Vol. **6151**, Emerging Lithographic Technologies X,* M. J. Lercel, Ed., 61513R, (2006).

[9] I. V. Fomenkov, D. C. Brandt, A. N. Bykanov, A. I. Ershov, W. N. Partlo, D. W. Myers, N. R. Böwering, G. O. Vaschenko, O. V. Khodykin, J. R. Hoffman, E. Vargas L., R. D. Simmons, J. A. Chavez, C. P. Chrobak, in: these proceedings, paper 6517-131 (2007).